CRYSTAL GROWTH & DESIGN

Article

pubs.acs.org/crystal

Rational Synthesis of Metal–Organic Framework Nanocubes and Nanosheets Using Selective Modulators and Their Morphology-Dependent Gas-Sorption Properties

Minh-Hao Pham,[†,§] Gia-Thanh Vuong,[†,§] Frédéric-Georges Fontaine,[‡,§] and Trong-On Do*[,†,§]

[†]Department of Chemical Engineering, [‡]Department of Chemistry, [§]Centre de Recherche sur les Propriétés des Interfaces et de Catalyse (CERPIC), Laval University, Quebec City, G1V 0A6, and Center in Green Chemistry and Catalysis (CVCC), Quebec, Canada

Supporting Information

ABSTRACT: Nanocubes and nanosheets of $[Cu_2(ndc)_2(dabco)]_n$ metal–organic framework (ndc = 1,4-naphthalene dicarboxylate; dabco = 1,4-diazabicyclo[2.2.2]-octane) were synthesized by using simultaneously acetic acid and pyridine or only pyridine, respectively, as selective modulators. This approach can tailor crystal growing on different directions for the size- and shape-controlled synthesis of metal–organic framework (MOF) nanocrystals whose structure is composed of two or more types of linkers using selective modulators. These MOF nanocrystals exhibit high crystallinity and higher CO_2 uptakes compared to that of the bulk MOF material or of the $[Cu_2(ndc)_2(dabco)]_n$ nanorods generated by using only acetic acid as the selective modulator, which may be due to the morphology effect on their gas sorption properties.

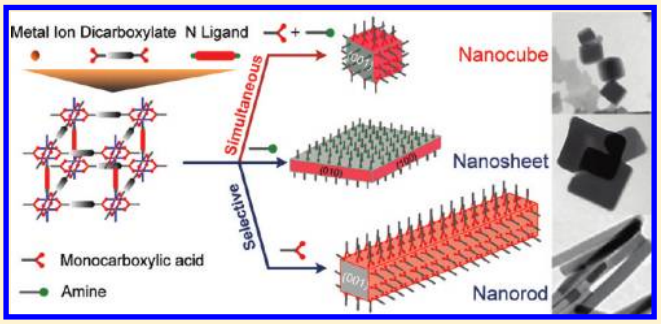

INTRODUCTION

Porous metal–organic framework (MOF) crystals have emerged as potential candidates in a number of practical applications such as drug delivery,[1] biomedical imaging,[2] sensing,[3] and gas adsorption.[4] In comparison with bulk materials, nanostructured MOFs exhibit unique shape- and size-dependent properties such as more accessible active sites, short diffusion pathways within the porous nanocrystals, and the ability to functionalize the external surfaces of MOF nanocrystals.[3b,5,6]

A number of synthetic methods have been reported for the preparation of MOF nanoparticles including microemulsions,[4b,7] surfactant-mediated methods,[8] microwave-assisted routes,[1a] and sonochemistry.[9] However, the precise control over the shape and size of MOF nanoparticles still remains challenging. Recently, selective coordination modulation approaches have been reported to synthesize MOF nanocrystals using a single capping reagent (so-called modulator).[10,11] For example, nanosized MOF-5 has been synthesized using *p*-perfluoromethylbenzenecarboxylate (pfmbc) as a modulator.[10a] Because MOF-5 is constructed from one type of linker (i.e., 1,4-benzenedicarboxylic acid) and Zn_4O clusters, it has an isotropic framework with only one coordination mode.[12] In the presence of the pfmbc, the carboxylate functionality of the modulator can impede the coordination between the zinc and the linkers to regulate the rate of the framework extension. Since the pfmbc also binds isotropically to the particle surface, such process can yield spherical/cubic MOF-5 nanocrystals. Tsuruoka et al. reported the synthesis of $[Cu_2(ndc)_2(dabco)]_n$ nanorods (ndc = 1,4-naphthalene dicarboxylate; dabco = 1,4-diazabicyclo[2.2.2]octane) using acetic acid as the modulator.[10b] Because the acetic acid selectively impedes the Cu-ndc coordination, nanorods are obtained solely.

The selective modulation methodology has been also used to control the shape and size of MOF crystals at the micrometer scale. Umemura et al. have recently reported the morphology-controlled synthesis of $[Cu_3(btc)_2]_n$ octahedron, cuboctahedron, and cubic microcrystals (btc = benzene-1,3,5-tricarboxylate) with a mean size of about 2 μm by changing the concentration of modulator (*n*-dodecanoic acid or lauric acid).[13] The control over the shape and size of MOF microcrystals was also achieved with additives that allow the protonation or deprotonation of the organic linkers. For example, the introduction of bases such as diethylamine, triethylamine, and acids such as acetic acid or HNO_3 allows adjusting the particle formation rate and the size and shape of microcrystals.[14]

Recently, we reported a new method for the synthesis of uniform MOF nanocrystals with controllable size and aspect ratio (length/width) using nonionic triblock copolymer F127 and acetic acid as stabilizing and deprotonation-controlling agents, respectively.[15] The alkylene oxide segments of the F127

Received: March 1, 2012
Revised: April 10, 2012
Published: April 24, 2012

ACS Publications © 2012 American Chemical Society

copolymer can coordinate metal ions and stabilize the MOF nuclei in the early stage of the formation of MOF nanocrystals, and acetic acid can control the deprotonation of carboxylic linkers during the synthesis, thus enabling the control of the nucleation rate, leading to tailored size and aspect ratio of nanocrystals.

Inspired by the methods for the synthesis of semiconductor nanocrystals,[16] crystalline MOFs constructed from two or more types of linkers (i.e., having different coordination modes), such as $[M_2(\text{dicarboxylate})_2(\text{N-ligand})]_n$,[17] could have controllable nanoscale size and shape using simultaneously different selective modulators. Herein, to demonstrate our approach we have chosen the three-dimensional $[Cu_2(ndc)_2(dabco)]_n$ MOF, composed of two distinct linkers,[17a] as a member of $[M_2(\text{dicarboxylate})_2(\text{N ligand})]_n$ MOF series. This MOF crystallizes in a tetragonal space group ($P4/mmm$), in which the dicarboxylate ligands (ndc) link the metal ions in the square paddle-wheel dicopper clusters to form two-dimensional square lattices, which are connected by the bidentate nitrogen pillar ligands (dabco) at the lattice points. Hence, the structure is dominated by two coordination modes: copper-ndc on the four ($h00$) and ($0k0$) facets and copper-dabco on two remaining ($00l$) facets. This allows modulating simultaneously the coordination modes of copper-ndc and copper-dabco by monocarboxylic acids and amines, respectively. Monocarboxylic acid, such as acetic acid, having the same carboxylate functionality as the ndc linker impedes the coordination interactions between copper and ndc in the [100] direction, whereas amine containing a nitrogen atom with a lone pair similar to that of dabco impedes the coordination between copper and dabco in the [001] direction. As a result, both the [100] and [001] directions of the crystal growth can be regulated to form nanocubes using both modulators (Scheme 1, Route 1), instead of using a single modulator: pyridine for nanosheets (Route 2) and acetic acid for nanorods (Route 3).

Scheme 1. Coordination Modulations toward $[M_2(\text{dicarboxylate})_2(\text{N ligand})]_n$ MOF Nanocrystals with Controlled Morphologies

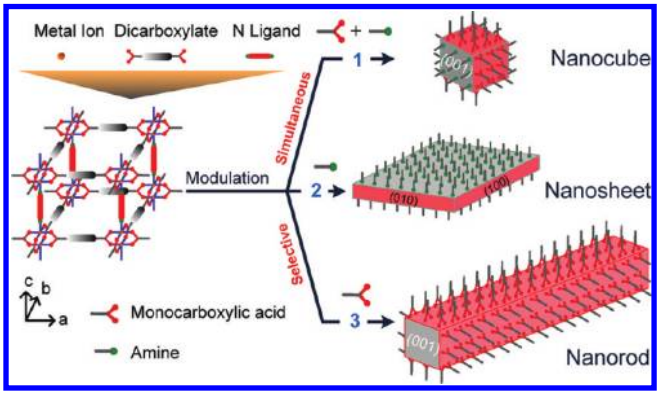

Route 1: Simultaneous modulation of metal-carboxylate and metal−nitrogen coordination modes using both monocarboxylic acid and amine to prepare nanocubes.
Route 2: Selective modulation of metal−nitrogen mode using only amine toward nanosheets.
Route 3: Selective modulation of metal-carboxylate mode using only monocarboxylic acid toward nanorods.

EXPERIMENTAL SECTION

Chemicals. Copper(II) acetate monohydrate (≥99%), 1,4-naphthalenedicarboxylic acid (94%), 1,4-diazabicyclo[2.2.2]octane (≥99%), pyridine (≥99%), and *N*,*N*-dimethylformamide (DMF, 99.8%) were purchased from Sigma-Aldrich. Acetic acid (99.7%) was purchased from Fisher Scientific. All chemicals were used as received without further purification.

Synthesis. For a typical synthesis of $[Cu_2(ndc)_2(dabco)]_n$ nanocubes, a solution of 70 mg of 1,4-naphthalenedicarboxylic acid (0.06 M), 18 mg of 1,4-diazabicyclo[2.2.2]octane (0.03 M), and 0.38 mL of pyridine (0.9 M) in 5 mL of DMF was poured into a solution of 90 mg of $Cu(CH_3COO)_2{\cdot}H_2O$ (0.06 M) and 0.26 mL of acetic acid (0.6 M) in 7.5 mL of DMF in a glass vial under vigorous stirring. The synthetic mixture was stirred for 30 min before being transferred into an autoclave and subsequently heated at 100 °C for 24 h. The resulting product was filtered, washed several times with anhydrous ethanol, and dried at 75 °C overnight.

The same process was applied to synthesizing $[Cu_2(ndc)_2(dabco)]_n$ nanosheets. In this synthesis, a solution of 70 mg of 1,4-naphthalenedicarboxylic acid (0.06 M), 18 mg of 1,4-diazabicyclo[2.2.2]octane (0.03 M), and 0.70 mL of pyridine (1.5 M) in 5 mL of DMF was first poured into a solution of 90 mg of $Cu(CH_3COO)_2{\cdot}H_2O$ (0.06 M) in 7.5 mL of DMF. The subsequent process was exactly the same as that for the nanocubes.

For the benchmark, the bulk $[Cu_2(ndc)_2(dabco)]_n$ material was also prepared. First, a solution of 70 mg of 1,4-naphthalenedicarboxylic acid (0.06 M) and 18 mg of 1,4-diazabicyclo[2.2.2]octane (0.03 M) in 5 mL of DMF was poured into a solution of 90 mg of $Cu(CH_3COO)_2{\cdot}H_2O$ (0.06 M) in 7.5 mL of DMF. The subsequent steps were performed the same as that for the nanocubes and nanosheets.

Characterization. Transmission electron microscopy (TEM) images were obtained using a JEOL JEM 1230 microscope operating at 120 kV. Samples for TEM measurements were prepared by depositing each drop of the dispersions of the products in anhydrous ethanol onto a carbon-coated copper grid (200 mesh). The excess of the solvent was wicked away with a filter paper, and the grids were then dried in air. Powder X-ray diffraction (XRD) patterns were collected on a Bruker SMART APEX II X-ray diffractometer with Cu Kα radiation (λ = 1.5406 Å) in the 2θ range 5 − 30° at a scan rate of 1.0° min^{-1}. Thermogravimetric analysis (TGA) was carried out with a Q5000 thermal analysis instrument (TGA Q5000) from room temperature to 600 °C with a heating rate of 5 °C min^{-1} under an air flow of 25 mL min^{-1}. The adsorption−desorption of N_2 at 77 K and of CO_2 at 273 K were performed with a Quantachrome Autosorb-1 system. The products were outgassed under a vacuum at 373 K overnight before the gas sorptions. The Brunauer−Emmett−Teller (BET) surface area was calculated from the experimental pressure range identified by established consistency criteria reported by Walton and Snurr for MOFs,[18] herein the 0.05−0.2 P/P_o range of linearity of the N_2 adsorption isotherm. The pore volume was calculated as the N_2 uptake at the relative pressure of 0.9.

RESULTS AND DISCUSSION

Nanocubes of $[Cu_2(ndc)_2(dabco)]_n$ MOF were achieved by using simultaneously acetic acid and pyridine as selective modulators. Figure 1 shows TEM images of a series of samples prepared with different pyridine concentrations, while keeping the same acetic acid concentration at 0.6 M. At pyridine concentrations less than 0.6 M, nanocubes along with nanobars and nanorods were observed (Figure 1a and see Supporting Information, Figure S1). However, at higher pyridine concentrations (≥0.6 M) only nanocubes were produced (Figure 1b−d). The three-dimensional shape of the MOF nanocrystals was determined from TEM images oriented differently toward the incident electron beam.[19] The size of nanocubes decreases slightly with increasing the pyridine

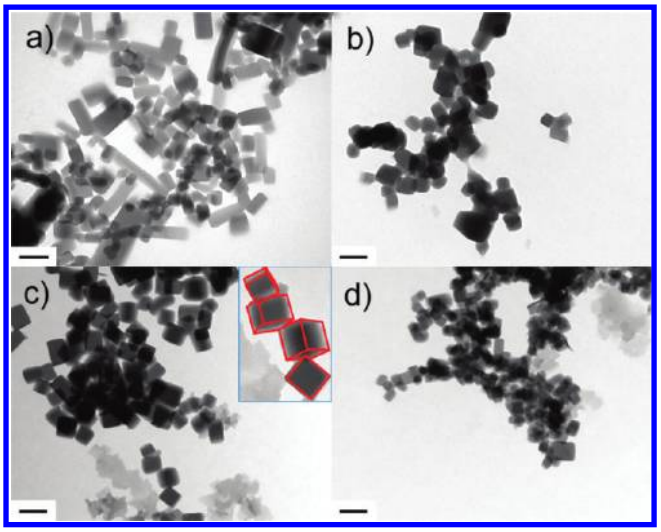

Figure 1. Morphology evolution of $[Cu_2(ndc)_2(dabco)]_n$ nanocrystals prepared at 0.6 M acetic acid with various concentrations of pyridine: (a) 0.3 M; (b) 0.6 M; (c) 0.9 M; and (d) 1.2 M. The scale bar is 200 nm.

concentration, from 100 ± 35 nm at 0.6 M to 80 ± 20 nm at 1.2 M pyridine. However, uniform size and well-defined nanocubes were observed at 0.9 M pyridine (Figure 1c).

In the presence of 1.5 M pyridine without acetic acid, the formation of nanosheets was observed (Figure 2 and see

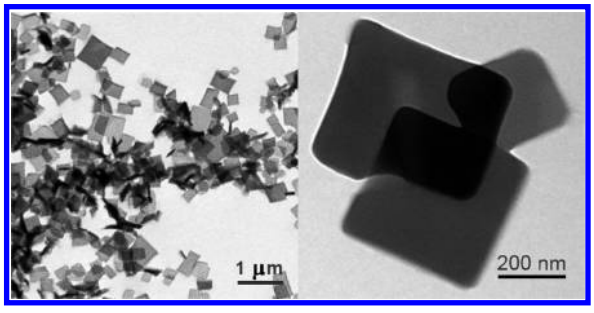

Figure 2. TEM images of $[Cu_2(ndc)_2(dabco)]_n$ nanosheets prepared in the presence of 1.5 M pyridine without acetic acid.

Supporting Information, Figure S2). This is attributed to the selective modulation of pyridine for the copper-dabco mode. On the contrary, in the absence of pyridine at the same acetic acid concentration (0.6 M), only nanorods were yielded (see Supporting Information, Figure S3) as previously reported by Kitagawa et al., due to the selective modulation of acetic acid for copper-ndc mode.[10b]

Therefore, the formation of the nanocubes in our approach suggests that pyridine has a role in modulating the copper-dabco coordination on the two (00*l*) facets and impedes the crystal growth in the [001] direction, whereas acetic acid plays a role in modulating the copper-ndc mode on the four remaining (*h*00) and (0*k*0) facets and thus suppresses the crystal growth in the [100] direction. As a result, the crystal growth in both the [100] and [001] directions is regulated simultaneously to yield nanocubes.

When the pyridine concentration was kept unchanged (e.g., 0.6 M) at acetic acid concentrations less than 0.6 M, nanocubes with nonuniform sizes along with nanobars were found (see Supporting Information, Figure S4a). However, at higher acetic acid concentrations (≥0.6 M), only nanocubes were yielded (Figure 1b and see Supporting Information, Figure S4b,c). The size of the nanocubes decreases slightly with an increasing concentration of acetic acid. It has been reported that a larger amount of the modulators enables a larger external surface area of the nanocrystals to be capped,[10b] leading to smaller nanocubes when prepared at higher pyridine and acetic acid concentrations.

The X-ray diffraction (XRD) patterns for a series of the nanocubes prepared by keeping unchanged the 0.6 M acetic acid concentration but varying the concentration of pyridine, along with the nanosheets fabricated with 1.5 M solution of pyridine in the absence of acetic acid, exhibit intense diffraction peaks that match those of the simulation, indicating highly crystalline nanomaterials (Figure 3). It is also noted that the

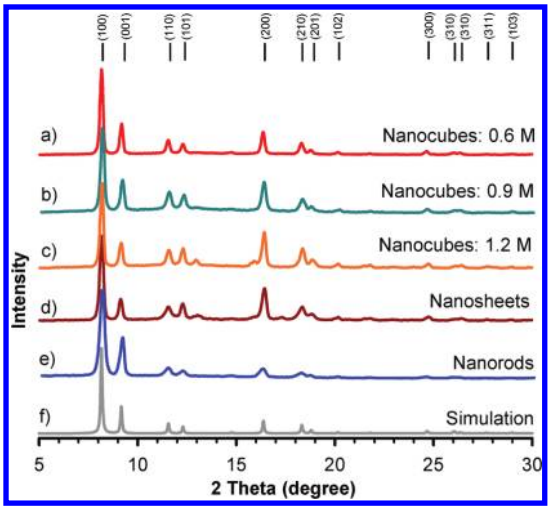

Figure 3. XRD patterns for $[Cu_2(ndc)_2(dabco)]_n$ nanocubes prepared by keeping the acetic acid concentration (0.6 M) unchanged with various concentrations of pyridine: (a) 0.6 M; (b) 0.9 M; (c) 1.2 M; (d) the nanosheets prepared at 1.5 M pyridine without acetic acid; (e) the nanorods prepared at 0.6 M acetic acid without pyridine and (f) the simulated pattern created from CIF file.[17a]

relative ratios of peak area for the (001) reflection of the nanocubes and of the nanosheets are smaller than that of the nanorods. This is attributed to the suppression of the crystal growth along the [001] direction of the nanocubes and the nanosheets in the presence of pyridine.

The adsorption and desorption of N_2 at 77 K and CO_2 at 273 K for the nanocubes prepared at 0.6 M acetic acid and 0.6 M pyridine, the nanosheets prepared at 1.5 M pyridine without acetic acid, and the nanorods prepared at 0.6 M acetic acid without pyridine are shown in Figure 4 and Table 1. The obtained results indicate that the BET surface area and pore volume of the nanomaterials are greater than those of the bulk MOF material. As seen in Figure 4b, the nanomaterials have a high CO_2 uptake at 273 K and 1 bar.[20] Interestingly, the nanocube and nanosheet samples show slightly higher CO_2 uptakes than that of the bulk and the nanorod materials at 273 K and 1 bar (Table 1); even the BET surface area and pore volume of the nanocube sample are lower than those of the nanorod one. Lee et al. have reported that the gas sorption property of MOF microcrystals can vary according to crystal morphology or exposed surfaces.[21] Therefore, in the case of $[Cu_2(ndc)_2(dabco)]_n$ nanocrystals, it is expected that the nature of the exposed crystal facets terminated by the different

dx.doi.org/10.1021/cg300297p | *Cryst. Growth Des.* 2012, 12, 3091−3095

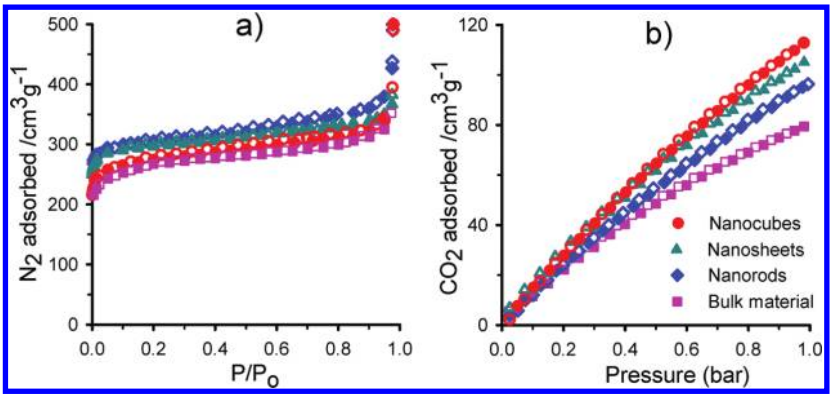

Figure 4. Gas adsorption (solid symbols)-desorption (open symbols) isotherms of N_2 at 77 K (a) and CO_2 at 273 K (b) for $[Cu_2(ndc)_2(dabco)]_n$ nanocubes prepared at 0.6 M acetic acid and 0.6 M pyridine (circles); for the nanosheets prepared at 1.5 M pyridine without acetic acid (triangles); for the nanorods prepared at 0.6 M acetic acid without pyridine (diamonds); and for the bulk MOF material (squares).

Table 1. Porosity and CO_2 Uptake of the Nanocrytals and the Bulk Material

	modulator concentration (M)				
sample	acetic acid	pyridine	BET surface area (m^2 g^{-1})	pore volume (cm^3 g^{-1})	CO_2 uptake at 1 bar, 273 K (mmol g^{-1})
nanocubes	0.6	0.6	1040	0.50	5.0
nanosheets	0	1.5	1175	0.54	4.8
nanorods	0.6	0	1180	0.56	4.3
bulk material	0	0	916	0.47	3.5

modulators and the orientation of the two porous channels of the MOF structure relative to these exposed facets will lead to a differentiation in N_2 and CO_2 uptakes. Thermogravimetric (TGA) profiles indicate the same thermal stability of the nanocubes, nanosheets, and nanorods, up to 270 °C (see Supporting Information, Figure S5).

To investigate the capability to modulate of other amines, including tertiary and primary amines, for the control of the morphology of the nanocrystals, we employed triethylamine, *n*-dodecylamine, *n*-octylamine, and methylamine while keeping the same 0.6 M acetic acid concentration. However, the introduction of these amines in the synthetic mixture did not completely yield cubic nanocrystals (Figure 5). This can be due to their weak competition with the dabco linker for interaction with copper dimers, these amines being worse ligands than pyridine. Moreover, these aliphatic amines could be protonated and rendered inactive by acetic acid.

For pyridine, the lone pair on its nitrogen atom is in the same plane and in the same direction with the dipole moment and conjugates with the π electrons of the aromatic ring; these may induce the nitrogen atom to compete with that of dabco linker for the coordination to the metal ions.[22] As seen in Figure 5, in the case of triethylamine with concentrations less than or equal to 0.6 M, a precipitate containing nanocubes along with nanobars was formed. However, higher concentrations of triethylamine only yielded a reddish orange solid probably

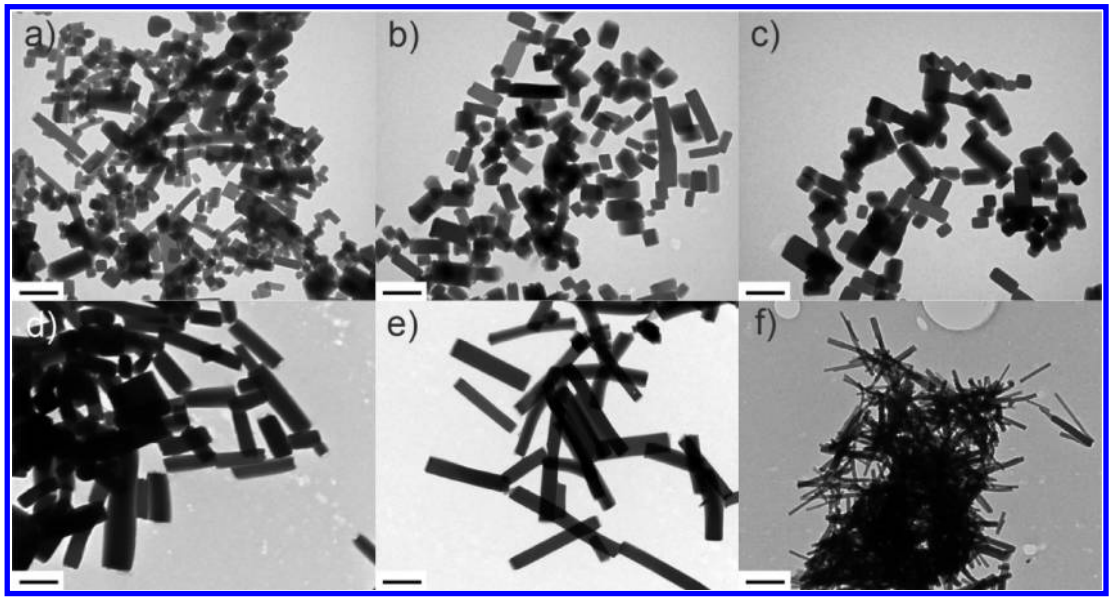

Figure 5. TEM images of $[Cu_2(ndc)_2(dabco)]_n$ nanocrystals fabricated in the presence of amines with 0.6 M acetic acid. (a–c) The different concentrations of triethylamine: (a) 0.1 M, (b) 0.3 M, (c) 0.6 M, (d) 0.1 M *n*-dodecylamine, (e) 0.1 M *n*-octylamine, and (f) 0.1 M methylamine. The scale bar is 500 nm.

dx.doi.org/10.1021/cg300297p | *Cryst. Growth Des.* 2012, 12, 3091–3095

caused by the reduction of copper ions. With the other amines, such reduction occurred at a much lower amine concentration (at 0.1 M) and the coordination modulation for copper-dabco mode eventually did not occur. As a consequence, only nanorods were produced.

CONCLUSION

We demonstrated the simple coordination modulation approach for the rational synthesis of nanocubes and nanosheets of $[Cu_2(ndc)_2(dabco)]_n$ MOF whose structures are composed of two coordination modes (metal-carboxylate and metal-amine modes) using simultaneously selective modulators (acetic acid and pyridine) or only one selective modulator (pyridine), respectively. The introduction of selective capping reagents that can cap different facets of growing MOF crystals allows us to prepare nanocrystals with controlled morphologies. In MOF chemistry, a large number of structures have crystal facets with intrinsically distinct chemical features that allow different functionalities to adhere selectively onto the facets.[23] Such methodology allows to tailor relative ratio of exposed crystal faces.

ASSOCIATED CONTENT

Supporting Information

TEM images, TGA curves for the nanocrystals prepared with different concentrations of pyridine and acetic acid. This material is available free of charge via the Internet at http://pubs.acs.org.

AUTHOR INFORMATION

Corresponding Author

*E-mail: Trong-On.Do@gch.ulaval.ca.

Notes

The authors declare no competing financial interest.

ACKNOWLEDGMENTS

The authors would like to thank the Natural Sciences and Engineering Research Council of Canada (NSERC) and Vietnam Ministry of Education and Training for a scholarship (to Minh-Hao Pham).

REFERENCES

(1) (a) Horcajada, P.; et al. *Nat. Mater.* **2010**, *9*, 172−178. (b) Rieter, W. J.; Pott, K. M.; Taylor, K. M. L.; Lin, W. *J. Am. Chem. Soc.* **2008**, *130*, 11584−11585. (c) Taylor-Pashow, K. M. L.; Rocca, J. D.; Xie, Z.; Tran, S.; Lin, W. *J. Am. Chem. Soc.* **2009**, *131*, 14261−14263.

(2) (a) McKinlay, A. C.; Morris, R. E.; Horcajada, P.; Férey, G.; Gref, R.; Couvreur, P.; Serre, C. *Angew. Chem., Int. Ed.* **2010**, *49*, 6260−6266. (b) Rieter, W. J.; Taylor, K. M. L.; An, H.; Lin, W.; Lin, W. *J. Am. Chem. Soc.* **2006**, *128*, 9024−9025. (c) deKrafft, K. E.; Xie, Z.; Cao, G.; Tran, S.; Ma, L.; Zhou, O. Z.; Lin, W. *Angew. Chem., Int. Ed.* **2009**, *48*, 9901−9904.

(3) (a) Allendorf, M. D.; Houk, R. J. T.; Andruszkiewicz, L.; Talin, A. A.; Pikarsky, J.; Choudhury, A.; Gall, K. A.; Hesketh, P. J. *J. Am. Chem. Soc.* **2008**, *130*, 14404−14405. (b) Rieter, W. J.; Taylor, K. M. L.; Lin, W. *J. Am. Chem. Soc.* **2007**, *129*, 9852−9853.

(4) (a) Nune, S. K.; Thallapally, P. K.; Dohnalkova, A.; Wang, C.; Liu, J.; Exarhos, G. *J. Chem. Commun.* **2010**, *46*, 4878−4880. (b) Tanaka, D.; Henke, A.; Albrecht, K.; Moeller, M.; Nakagawa, K.; Kitagawa, S.; Groll, J. *Nat. Chem.* **2010**, *2*, 410−416.

(5) (a) Carné, A.; Carbonell, C.; Imaz, I.; Maspoch, D. *Chem. Soc. Rev.* **2011**, *40*, 291−305. (b) Hui, J. K.-H.; MacLachlan, M. J. *Coord. Chem. Rev.* **2010**, *254*, 2363−2390. (c) Lin, W.; Rieter, W. J.; Taylor, K. M. L. *Angew. Chem., Int. Ed.* **2009**, *48*, 650−658. (d) Uemura, T.; Kitagawa, S. *Chem. Lett.* **2005**, *34*, 132−137.

(6) Taylor, K. M. L.; Rieter, W. J.; Lin, W. *J. Am. Chem. Soc.* **2008**, *130*, 14358−14359.

(7) Diring, S.; Furukawa, S.; Takashima, Y.; Tsuruoka, T.; Kitagawa, S. *Chem. Mater.* **2010**, *22*, 4531−4538.

(8) (a) Uemura, T.; Kitagawa, S. *J. Am. Chem. Soc.* **2003**, *125*, 7814−7815. (b) Uemura, T.; Ohba, M.; Kitagawa, S. *Inorg. Chem.* **2004**, *43*, 7339−7345.

(9) Qiu, L. G.; Li, Z. Q.; Wu, Y.; Wang, W.; Xu, T.; Jiang, X. *Chem. Commun.* **2008**, 3642−3644.

(10) (a) Hermes, S.; Witte, T.; Hikov, T.; Zacher, D.; Bahnmuller, S.; Langstein, G.; Huber, K.; Fischer, R. A. *J. Am. Chem. Soc.* **2007**, *129*, 5324−5325. (b) Tsuruoka, T.; Furukawa, S.; Takashima, Y.; Yoshida, K.; Isoda, S.; Kitagawa, S. *Angew. Chem., Int. Ed.* **2009**, *48*, 4739−4743.

(11) (a) Horcajada, P.; Serre, C.; Grosso, D.; Boissiere, C.; Perruchas, S.; Sanchez, C.; Férey, G. *Adv. Mater.* **2009**, *21*, 1931−1935. (b) Guo, H.; Zhu, Y.; Qiu, S.; Lercher, J. A.; Zhang, H. *Adv. Mater.* **2010**, *22*, 4190−4192.

(12) Li, H.; Eddaoudi, M.; O'Keeffe, M.; Yaghi, O. M. *Nature* **1999**, *402*, 276−279.

(13) Umemura, A.; Diring, S.; Furukawa, S.; Uehara, H.; Tsuruoka, T.; Kitagawa, S. *J. Am. Chem. Soc.* **2011**, *133*, 15506−15513.

(14) (a) Li, Y. S.; Bux, H.; Feldhoff, A.; Li, G. L.; Yang, W. S.; Caro, J. *Adv. Mater.* **2010**, *22*, 3322−3326. (b) Wang, K.; Geng, Z.; Yin, Y.; Ma., X.; Wang, Z. *CrystEngComm* **2011**, *13*, 5100−5104. (c) Lu, Y.; Cao, H.; Zhang, S.; Zhang, X. *J. Mater. Chem.* **2011**, *21*, 8633−8639.

(15) Pham, M. H.; Vuong, G. T.; Vu, A. T.; Do, T. O. *Langmuir* **2011**, *27*, 15261−15267.

(16) (a) Dinh, C. T.; Nguyen, T. D.; Kleitz, F.; Do, T. O. *ACS Nano* **2009**, *3*, 3737−3743. (b) Yin, Y.; Alivisatos, A. P. *Nature* **2005**, *437*, 664−670.

(17) (a) Furukawa, S.; Hirai, K.; Nakagawa, K.; Takashima, Y.; Matsuda, R.; Tsuruoka, T.; Kondo, M.; Haruki, R.; Tanaka, D.; Sakamoto, H.; Shimomura, S.; Sakata, O.; Kitagawa, S. *Angew. Chem., Int. Ed.* **2009**, *48*, 1766−1770. (b) Tanaka, D.; Higuchi, M.; Horike, S.; Matsuda, R.; Kinoshita, Y.; Yanai, N.; Kitagawa, S. *Chem. Asian J.* **2008**, *3*, 1343−1349. (c) Dybtsev, D. N.; Chun, H.; Kim, K. *Angew. Chem., Int. Ed.* **2004**, *43*, 5033−5036. (d) Ma, B.-Q.; Mulfort, K. L.; Hupp, J. T. *Inorg. Chem.* **2005**, *44*, 4912−4914. (e) Seki, K.; Mori, W. *J. Phys. Chem. B* **2002**, *106*, 1380−1385. (f) Chun, H.; Dybtsev, D. N.; Kim, H.; Kim, K. *Chem.—Eur. J.* **2005**, *11*, 3521−3529.

(18) Walton, K. S.; Snurr, R. Q. *J. Am. Chem. Soc.* **2007**, *129*, 8552−8556.

(19) (a) Lebedev, O. I.; Millange, F.; Serre, C.; Tendeloo, G. V.; Férey, G. *Chem. Mater.* **2005**, *17*, 6525−6527. (b) Pham, M. H.; Vuong, G. T.; Fontaine, F. G.; Do, T. O. *Cryst. Growth Des.* **2012**, *12*, 1008−1013.

(20) (a) Millward, A. R.; Yaghi, O. M. *J. Am. Chem. Soc.* **2005**, *127*, 17998−17999. (b) An, J.; Geib, S. J.; Rosi, N. L. *J. Am. Chem. Soc.* **2010**, *132*, 38−39.

(21) Lee, H. J.; Cho, W.; Jung, S.; Oh, M. *Adv. Mater.* **2009**, *21*, 674−677.

(22) Yang, Y. S.; Hsu, W. Y.; Lee, H. F.; Huang, Y. C.; Yeh, C. S. *J. Phys. Chem. A* **1999**, *103*, 11287−11292.

(23) (a) Biemmi, E.; Scherb, C.; Bein, T. *J. Am. Chem. Soc.* **2007**, *129*, 8054−8055. (b) Scherb, C.; Schodel, A.; Bein, T. *Angew. Chem., Int. Ed.* **2008**, *47*, 5777−5779. (c) Liu, B.; Ma, M.; Zacher, D.; Bétard, A.; Yusenko, K.; Metzler-Nolte, N.; Woll, C.; Fischer, R. A. *J. Am. Chem. Soc.* **2011**, *133*, 1734−1737.

Supporting Information

Rational Synthesis of Metal-Organic Framework Nanocubes and Nanosheets Using Selective Modulators and Their Morphology-Dependent Gas-Sorption Properties

Minh-Hao Pham,[†,§] Gia-Thanh Vuong,[†,§] Frédéric-Georges Fontaine,[‡,§] and Trong-On Do[*,†,§]

[†]*Department of Chemical Engineering,* [‡]*Department of Chemistry*

[§]*Centre de Recherche sur les Propriétés des Interfaces et de Catalyse (CERPIC)*

Laval University, Quebec City, Quebec, G1V 0A6, Canada

E-mail: Trong-On.Do@gch.ulaval.ca

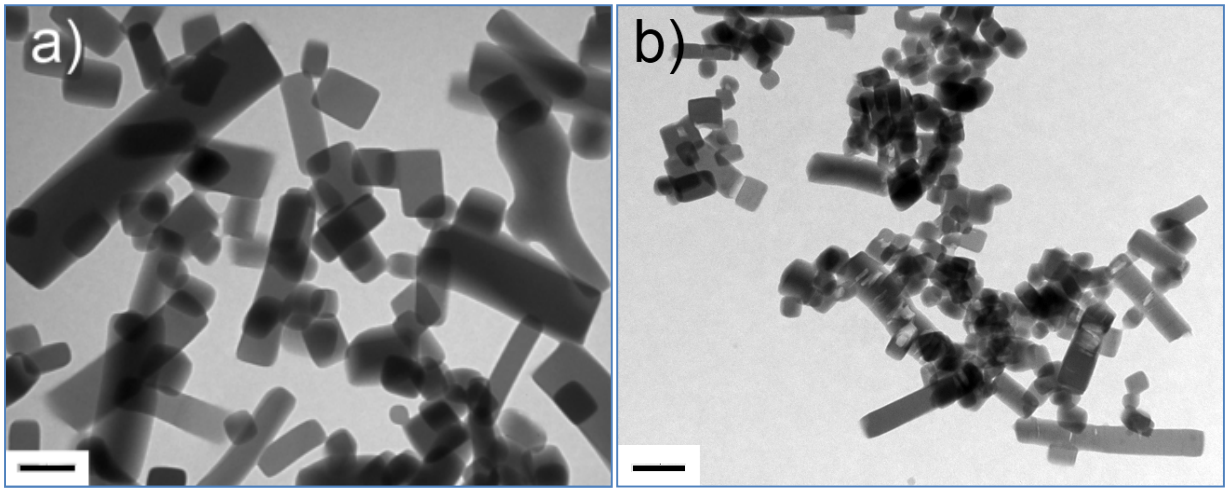

Figure S1. TEM images of $[Cu_2(ndc)_2(dabco)]_n$ nanocrystals prepared at 0.6 M acetic acid with the concentration of pyridine at 0.1 M (a) and 0.45 M (b). The scale bar is 200 nm.

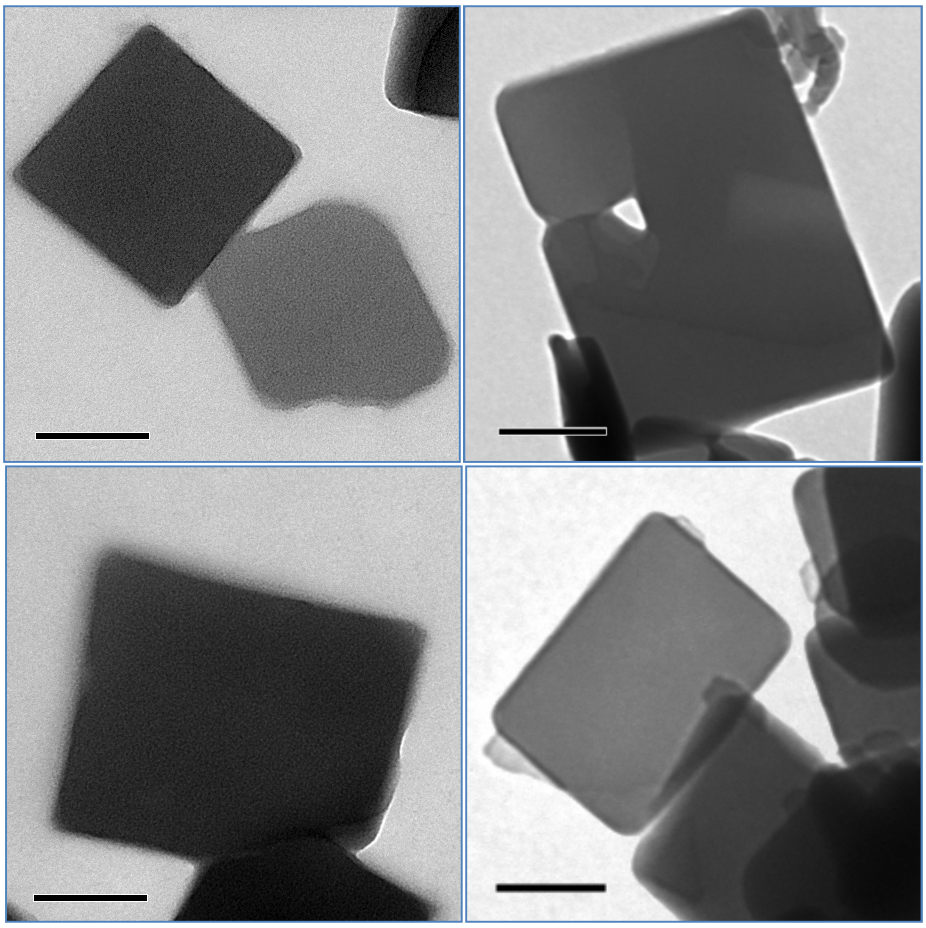

Figure S2. TEM images of $[Cu_2(ndc)_2(dabco)]_n$ nanosheets prepared in the absence of acetic acid with the concentration of pyridine at 1.5 M. The scale bar is 200 nm.

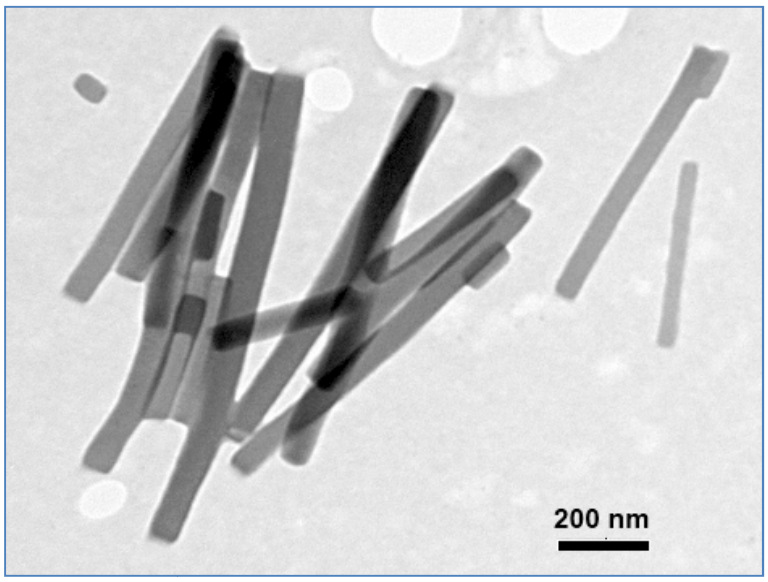

Figure S3. TEM image of $[Cu_2(ndc)_2(dabco)]_n$ square nanorods prepared at 0.6 M acetic acid in the absence of pyridine.

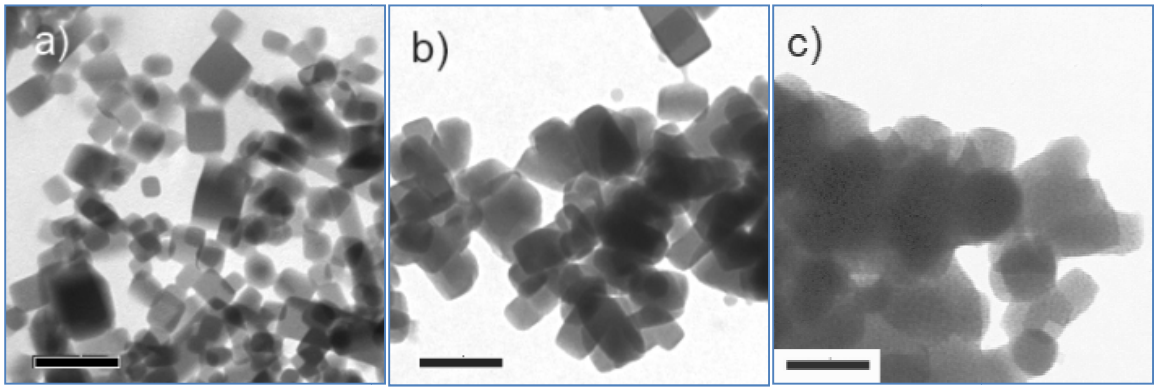

Figure S4. TEM images of $[Cu_2(ndc)_2(dabco)]_n$ nanocrystals prepared at 0.6 M pyridine with the concentration of acetic acid at 0.3 M (a); 0.9 M (b) and 1.2 M (c). The scale bar is 200 nm.

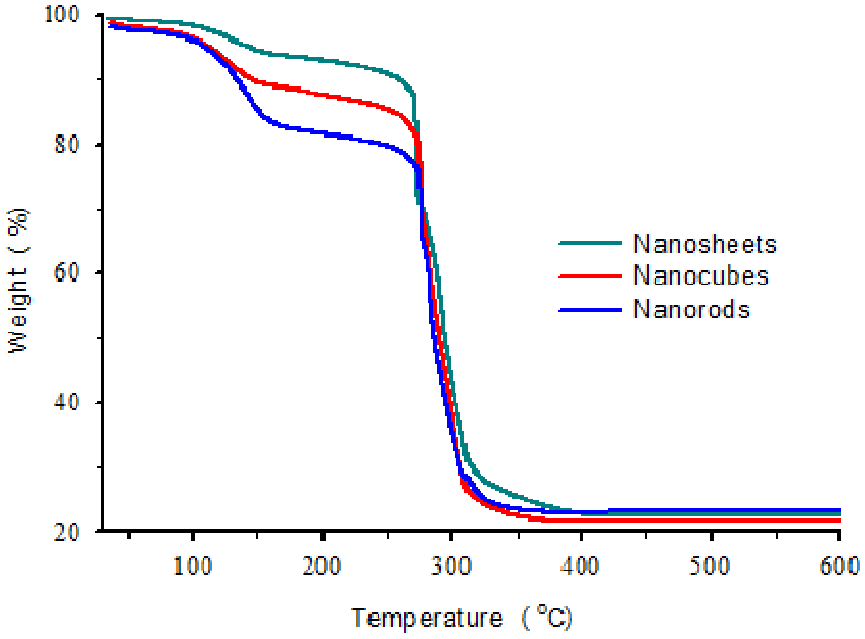

Figure S5. TGA curves for $[Cu_2(ndc)_2(dabco)]_n$ nanocubes prepared at 0.6 M acetic acid with 0.6 M pyridine, for the nanosheets fabricated at 1.5 M pyridine in the absence of acetic acid and for the nanorods prepared by 0.6 M acetic acid without pyridine.

Full author list of Ref. 1a:

Horcajada, P.; Chalati, T.; Serre, C.; Gillet, B.; Sebrie, C.; Baati, T.; Eubank, J. F.; Heurtaux, D.; Clayette, P.; Kreuz, C.; Chang, J. S.; Hwang, Y. K.; Marsaud, V.; Bories, P. N.; Cynober, L.; Gil, S.; Férey, G.; Couvreur P.; Gref, R.